Available online at www.sciencedirect.com

SCIENCE DIRECT®

Journal of Solid State Chemistry 177 (2004) 1346–1351

JOURNAL OF SOLID STATE CHEMISTRY

http://elsevier.com/locate/jssc

Intercalation of KCl into layered neptunyl and plutonyl iodates☆

Amanda C. Bean,[a,*] Brian L. Scott,[b] Thomas E. Albrecht-Schmitt,[c] and Wolfgang Runde[b]

[a] *Nuclear Materials Technology, Los Alamos National Laboratory, P.O. Box 1663 MS J514, Los Alamos, NM 87545, USA*
[b] *Chemistry Division, Los Alamos National Laboratory, Los Alamos, NM 87545, USA*
[c] *Department of Chemistry, Auburn University, Auburn, AL 36849, USA*

Received 21 August 2003; received in revised form 27 October 2003; accepted 6 November 2003

Abstract

The hydrothermal reaction of Np(IV) or Pu(IV) with KIO_4 and CsCl at 180°C for 1 day results in the formation of $NpO_2(IO_3)_2 \cdot 0.5KCl \cdot 3.25H_2O$ (**1**) or $PuO_2(IO_3)_2 \cdot 0.5KCl \cdot 2.5H_2O$ (**2**). The neutral layers in compounds **1** and **2** are isostructural with $NpO_2(IO_3)_2 \cdot H_2O$ and $PuO_2(IO_3)_2 \cdot H_2O$, respectively. The Np and Pu centers are found in distorted pentagonal bipyramidal $[AnO_7]$ environments that are formed from the ligation of NpO_2^{2+} or PuO_2^{2+} cations by iodate anions. There are two crystallographically unique pyramidal iodate anions in **1** and **2**. One of these anions utilizes all three oxygen atoms to simultaneously bridge three neptunyl or plutonyl units. The second anion only bridges two actinyl units and has a terminal oxo atom. The bridging of the actinyl cations by iodate anions creates neutral $^{2}_{\infty}[AnO_2(IO_3)_3]$ (An = Np, Pu) sheets that are separated by K^+ cations, Cl^- anions, and water molecules. Crystallographic data (203 K, Mo$K\alpha$, $\lambda = 0.71073$): **1**, monoclinic, space group $C2/c$, $a = 21.537(5)$ Å, $b = 11.670(3)$ Å, $c = 7.315(2)$ Å, $\beta = 93.033(4)°$, $Z = 4$, $R(F) = 5.43\%$ for 136 parameters with 1309 reflections with $I > 2\sigma(I)$; **2**, monoclinic, space group $C2/c$, $a = 21.570(4)$ Å, $b = 11.656(2)$ Å, $c = 7.348(2)$ Å, $\beta = 94.00(3)$, $Z = 4$, $R(F) = 4.92\%$ for 148 parameters with 1317 reflections with $I > 2\sigma(I)$.

Keywords: Actinide; Iodate; Crystal structure; Hydrothermal; Plutonyl remarks

---

1. Introduction

The remarkable insolubility of transuranium iodates was discovered some 60 years ago and was used for the separation of plutonium from fission products by precipitation at low pH [1–4]. In the first report on the chemistry of plutonium, published in 1944, disclosure was made of the formation of a pink amorphous precipitate of $Pu(IO_3)_4$ from KIO_3–HNO_3 solutions [5]. Thermogravimetric studies indicated that this pink precipitate probably incorporated HIO_3 as well [6]. Pu(IV) iodate was credited for its applications in analytical separations and purifications because of its aforementioned low solubility in solutions as strong as 6 M HNO_3 [5]. In addition, a Pu(III) iodate, $Pu(IO_3)_3$, was found to precipitate as a tan solid upon the addition of aqueous iodate solutions, such as KIO_3, to Pu^{3+} solutions [1]. From these fundamental discoveries stemmed further interest in the application of plutonium separations using iodate. For example, an iodate cycle was used in the past for the purification of plutonium [2]. Shortly thereafter, an iodate method was used for the purification and separation of plutonium from the iodates of alkali metals and lanthanides [3], as well as from uranium and various other fission products [4].

^{129}I, a key fission product, has been found in soil and grass samples surrounding a nuclear reprocessing plant and has been suggested to exist as a variety of iodine species, including IO_3^- [7,8]. Current interest in iodate can then be coupled with growing concerns of actinide migration in the environment and their relevance as long-term contributors to radioactive dose in nuclear waste repositories [9,10]. Therefore, it is important to evaluate the reactions of actinides with fission-product radionuclides, such as ^{129}I. In addition to fundamental interests in the structural chemistry of actinide iodates, we have expanded on the uranyl iodate system [11–15] to

---

☆Further details of the crystal structure investigation may be obtained from the Fachinformationzentrum Karlsruhe, D-76344 Eggenstein-Leopoldshafen, Germany (Fax: (+49)7247-808-666; E-mail: crysdata@fiz-karlsruhe.de) on quoting depository numbers CSD 413331 and 413332.

*Corresponding author. Fax: +1-505-665-4955.
E-mail address: bean@lanl.gov (A.C. Bean).

0022-4596/$ - see front matter © 2003 Elsevier Inc. All rights reserved.
doi:10.1016/j.jssc.2003.11.011

include the transuranium elements neptunium and plutonium that also exist in nuclear waste.

The synthetic and structural chemistry of the transuranic elements has fallen behind their uranium counterparts, in part, because of the limited facilities that exist to investigate such materials, i.e., long-lived alpha-emitters, and their diminished accessibility. Recently, hydrothermal methods have been used to safely probe the chemistry of neptunium and plutonium with iodate, and $PuO_2(IO_3)_2 \cdot H_2O$ [16], $NpO_2(IO_3)_2(H_2O)$ [17], $NpO_2(IO_3)_2 \cdot H_2O$ [17] were prepared as single crystals and structurally characterized. Herein we report the preparation and crystal chemistry of $NpO_2(IO_3)_2 \cdot 0.5KCl \cdot 3.25H_2O$ (**1**) and $PuO_2(IO_3)_2 \cdot 0.5KCl \cdot 2.5H_2O$ (**2**), which contain neptunyl and plutonyl iodate layers found in $AnO_2(IO_3)_2 \cdot H_2O$ (An = Np, Pu) [17] intercalated by KCl and water molecules.

2. Experimental

2.1. Syntheses

KIO_4 (99.9%, Fisher) and CsCl (99.9%, Aldrich) were used as received. A $^{237}Np(IV)$ stock solution (0.1 M) was prepared by dissolution of $^{237}NpO_2$ in 3 M HCl, followed by a subsequent precipitation with 1 M NaOH and dissolution of the washed precipitate in 0.5 M HCl. The $^{239}Pu(IV)$ stock (0.17 M) was prepared by dissolution of Pu^0 in nitric acid solution, which was placed on an anion exchange column and eluted with 0.5 M HCl. Distilled and Millipore filtered water with a resistance of 17.2 MΩ was used in all reactions. *Samples containing transuranic elements should be handled with caution owing to their inhalation hazards.* Reactions were carried out using 10-mL PTFE-lined autoclaves with a reaction temperature of 180°C for 1 day. After this time, the autoclaves were cooled at 13°C/h to 25°C. The crystals were placed in a small vial and the mother liquor was removed. Yield for **1** appeared to be produced in high yield (estimated 90% by neptunium) from evidence of a clear solution over pure product. Yield for **2** was undetermined owing to difficulty in separation of products. The Raman spectra were collected on a Nicolet Magna 560 FT-IR/Raman spectrometer. Approximately 5 mg crystalline samples in doubly contained NMR tubes were used for Raman spectroscopy studies.

2.2. Synthesis of $NpO_2(IO_3)_2 \cdot 0.5KCl \cdot 3.25H_2O$ (1)

A Teflon liner were loaded with $^{237}Np(IV)$ (200 μL, 0.02 mmol) stock solution, KIO_4 (43.4 mg, 0.19 mmol), and CsCl (53.2 mg, 0.32 mmol) followed by 600 μL of deionized water. The autoclave was sealed, doubly contained in two heat-sealed Teflon bags and placed in a box furnace. The product consisted of clear solution over light green diamond-shaped crystals of **1** and excess salt crystals. Raman (cm^{-1}): $v(I-O)$ 786 (w, br); 761 (s); 746 (s).

2.3. Synthesis of $PuO_2(IO_3)_2 \cdot 0.5KCl \cdot 2.5H_2O$ (2)

A Teflon liner were loaded with $^{239}Pu(IV)$ (200 μL, 0.034 mmol) stock solution, KIO_4 (74.4 mg, 0.32 mmol), and CsCl (70.1 mg, 0.42 mmol) followed by 500 μL of deionized water. The autoclave was sealed, doubly contained in two-healed sealed Teflon bags and placed in a box furnace. The product consisted of clear solution over orange diamond-shaped crystals of **2,** and orange columns and red blocks of $PuO_2(IO_3)_2 \cdot H_2O$ [16]. Owing to the mixture of products, **2** could not be separated efficiently for Raman.

2.3.1. Crystallographic studies

Suitable crystals of $NpO_2(IO_3)_2 \cdot 0.5KCl \cdot 3.25H_2O$ (**1**) ($0.04 \times 0.10 \times 0.14\,mm^3$) and $PuO_2(IO_3)_2 \cdot 0.5KCl \cdot 2.5H_2O$ (**2**) ($0.06 \times 0.25 \times 0.25\,mm^3$) were mounted in glass capillaries after coating with epoxy. The capillaries were then coated with clear nail polish as a third form of containment. The crystals were placed on a Bruker P4/CCD/PC X-ray diffractometer and cooled to 203 K using a Bruker LT-2 low-temperature device. The data were collected using a sealed, graphite monochromatic Mo$K\alpha$ X-ray source. A hemisphere of data was collected using a combination of φ and ω scans with 30-s frame exposures and 0.3° frame widths. Data collection and initial indexing and cell refinement were handled using SMART software [18]. Frame integration and final cell parameter calculations were carried out using SAINT software [18]. The data were corrected for absorption using SADABS for **1** and **2** because the geometry of this instrument prevents complete face-indexing [18]. In addition, a ψ-scan correction was also applied to **1**. The program suite SHELXTL was used for space group determination (XPREP), structure solution (XS), and refinement (XL) [19].

Direct methods was used to determine heavy atom positions and the final refinement included anisotropic displacement parameters for all atoms, excluding the water oxygen atom in **1**, and a secondary extinction parameter. The ISOR command was used to refine O(1), O(2), O(4), O(5w) and K(1) in **1** and O(5), O(1w), O(2w), O(4w), K(2) and Cl(1) in **2** to refine these atoms anisotropically. The minimum and maximum transmission factors are 0.075 and 0.478 for **1** and 0.020 and 0.391 for **2**. The merging R factors before the absorption corrections for **1** and **2** were 0.074 and 0.245, respectively. The final converged refinements resulted in $R_1 = 0.054$ and $wR_2 = 0.137$ based on 1227 unique reflections for **1** and $R_1 = 0.049$ and $wR_2 = 0.125$ based on 1307 unique reflections for **2**. All atoms are fully occupied with the

Table 1
Crystallographic data for $NpO_2(IO_3)_2 \cdot 0.5KCl \cdot 3.25H_2O$ (**1**) and $PuO_2(IO_3)_2 \cdot 0.5KCl \cdot 2.5H_2O$ (**2**)

Formula	$NpO_2(IO_3)_2 \cdot 0.5KCl \cdot 3.25H_2O$ (**1**)	$PuO_2(IO_3)_2 \cdot 0.5KCl \cdot 2.5H_2O$ (**2**)
Formula mass (amu)	708.07	698.08
Color and habit	Light green diamond-shaped	Orange diamond-shaped
Crystal system	Monoclinic	Monoclinic
Space group	*C*2/*c*	*C*2/*c*
a (Å)	21.537(5)	21.570(4)
b (Å)	11.670(3)	11.656(2)
c (Å)	7.315(2)	7.348(2)
α (deg)	90	90
β (deg)	93.033(4)°	94.00(3)°
γ (deg)	90	90
V (Å^3)	1836.0(7)	1842.9(6)
Z	4	4
T (°C)	−70	−70
λ (Å)	0.71073	0.71073
ρ_{calcd} (g cm^{-3})	4.805	5.032
μ(Mo$K\alpha$) (cm^{-1})	184.31	156.51
$R(F)$ for $F_o^2 > 2\sigma(F_o^2)$[a]	0.0543	0.0492
$R_w(F_o^2)$[b]	0.1374	0.1253

[a] $R(F) = \sum||F_o| - |F_c||/\sum|F_o|$.
[b] $R_w(F_o^2) = [\sum[w(F_o^2 - F_c^2)^2]/\sum wF_o^4]^{1/2}$.

Table 2
Atomic coordinates and equivalent isotropic displacement parameters for $NpO_2(IO_3)_2 \cdot 0.5KCl \cdot 3.25H_2O$ (**1**)

Atom	x	y	z	U_{eq} (Å^2)[a]	Occupancy
Np(1)	0.3538(1)	−0.7238(1)	0.2049(1)	0.013(1)	1.00
I(1)	0.3177(1)	−0.3941(1)	0.2054(2)	0.020(1)	1.00
I(2)	0.3371(1)	−0.0337(1)	0.0871(2)	0.023(1)	1.00
O(1)	0.2730(7)	−0.7186(11)	0.1849(19)	0.020(3)	1.00
O(2)	0.4330(8)	−0.7279(11)	0.2286(19)	0.025(4)	1.00
O(3)	0.3399(7)	−0.9029(12)	0.3566(17)	0.020(3)	1.00
O(4)	0.3648(7)	−0.5224(12)	0.2029(18)	0.020(3)	1.00
O(5)	0.3634(6)	−0.3255(13)	0.3962(19)	0.022(3)	1.00
O(6)	0.3540(7)	−0.3106(13)	0.0290(19)	0.026(3)	1.00
O(7)	0.3560(7)	0.1085(12)	0.0070(17)	0.019(3)	1.00
O(8)	0.2513(8)	−0.0192(14)	0.0730(20)	0.035(4)	1.00
Cl(1)	0.5134(4)	−0.1404(12)	0.1387(16)	0.023(2)	0.50
K(1)	0.5000	0.5000	0	0.038(3)	1.00
O(2W)	0.5200(20)	−0.0850(50)	0.0880(70)	0.003(12)	0.25
O(3W)	0.5042(13)	0.5180(20)	0.0670(30)	0.038(6)	1.00
O(4W)	0.4470(30)	−0.0570(50)	0.1290(80)	0.065(16)	0.50
O(5W)	0.5000	0.0290(40)	0.2500	0.098(13)	1.00
O(1W)	0.5000	−0.2988(14)	0.2500	0.002(3)	1.00
O(6W)	0.4620(30)	−0.0590(60)	0.0700(90)	0.078(19)	0.50

[a] U_{eq} is defined as one-third of the trace of the orthogonalized U_{ij} tensor.

exception of Cl(1), and water oxygens, O(1w), O(2w), O(4w), O(5w), and O(6w) in **1** and Cl(1), O(2w), and O(4w) in **2**. Some crystallographic details are listed in Table 1 and atomic coordinates are in Tables 2 and 3.

3. Results and discussion

3.1. Structures

The neutral layers found in $NpO_2(IO_3)_2 \cdot 0.5KCl \cdot 3.25H_2O$ (**1**) and $PuO_2(IO_3)_2 \cdot 0.5KCl \cdot 2.5H_2O$ (**2**) have the same topologies as $NpO_2(IO_3)_2 \cdot H_2O$ and $PuO_2(IO_3)_2 \cdot H_2O$, which were recently reported by our group [16,17]. Compounds **1** and **2** contain neutral ${}^{2}_{\infty}[AnO_2(IO_3)_2]$ (An = Np, Pu) layers that are separated by K^+ cations, Cl^- anions, and H_2O molecules, as shown in Fig. 1. These sheets are composed of pentagonal bipyramidal $[AnO_7]$ units connected by bridging pyramidal IO_3^- anions. The AnO_2^{2+} moiety, common for hexavalent actinides, is found as the *trans*-dioxo cation, and oxygen atoms from the iodate anions occupy the five equatorial sites, completing the coordination in the $[AnO_7]$ units (Fig. 2). All five iodate anions

Table 3
Atomic coordinates and equivalent isotropic displacement parameters for $PuO_2(IO_3)_2 \cdot 0.5KCl \cdot 2.5H_2O$ (**2**)

Atom	x	y	z	U_{eq} (Å^2)[a]	Occupancy
Pu(1)	0.3544(1)	−0.7247(1)	0.2085(2)	0.015(1)	1.00
I(1)	0.3188(1)	−0.3939(1)	0.2067(2)	0.023(1)	1.00
I(2)	0.3360(1)	−0.0336(1)	0.0876(2)	0.025(1)	1.00
O(1)	0.2736(7)	−0.7173(12)	0.1810(20)	0.026(3)	1.00
O(2)	0.4347(7)	−0.7326(13)	0.2390(19)	0.028(4)	1.00
O(3)	0.3393(7)	−0.9058(12)	0.3555(20)	0.025(3)	1.00
O(4)	0.3652(7)	−0.5218(13)	0.2020(20)	0.024(3)	1.00
O(5)	0.3647(7)	−0.3257(13)	0.4010(20)	0.027(3)	1.00
O(6)	0.3540(7)	−0.3105(13)	0.0290(20)	0.028(4)	1.00
O(7)	0.3560(7)	−0.1101(12)	0.0098(19)	0.024(3)	1.00
O(8)	0.2511(8)	−0.0181(14)	0.0730(20)	0.036(4)	1.00
Cl(1)	0.5158(4)	−0.1376(7)	0.1393(10)	0.008(2)	0.50
O(1W)	0.5000	1.3070(20)	0.7500	0.034(5)	1.00
O(2W)	0.6320(40)	−0.2770(70)	−0.1890(120)	0.070(40)	0.50
O(3W)	0.3731(12)	−0.0426(18)	−0.4090(30)	0.045(5)	1.00
O(4W)	0.5441(14)	−0.0600(30)	0.3990(40)	0.028(7)	0.50
K(1)	0.5000	0.5000	0	0.014(1)	1.00

[a] U_{eq} is defined as one-third of the trace of the orthogonalized U_{ij} tensor.

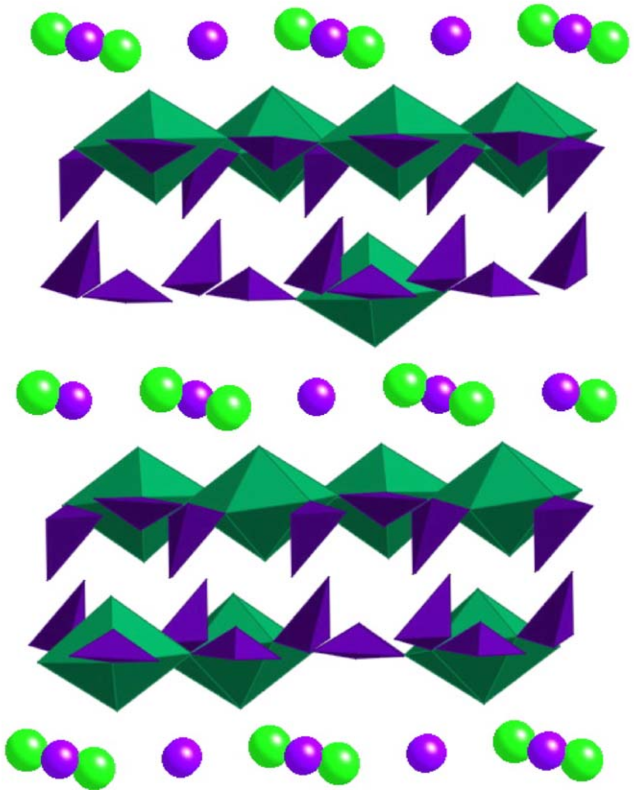

Fig. 1. A view of the structure of **1** and **2** down the *ac*-plane illustrating two neutral parallel layers of $[AnO_2(IO_3)_2]$ (An = Np, Pu) separated by K^+ (purple) and Cl^- (bright green) atoms. Interlayer water molecules have been omitted for clarity.

surrounding the $[AnO_7]$ polyhedra serve to bridge the units in two different coordination modes to form the two-dimensional sheets that run in the *bc* plane for **1** and **2**, as depicted in Fig. 3.

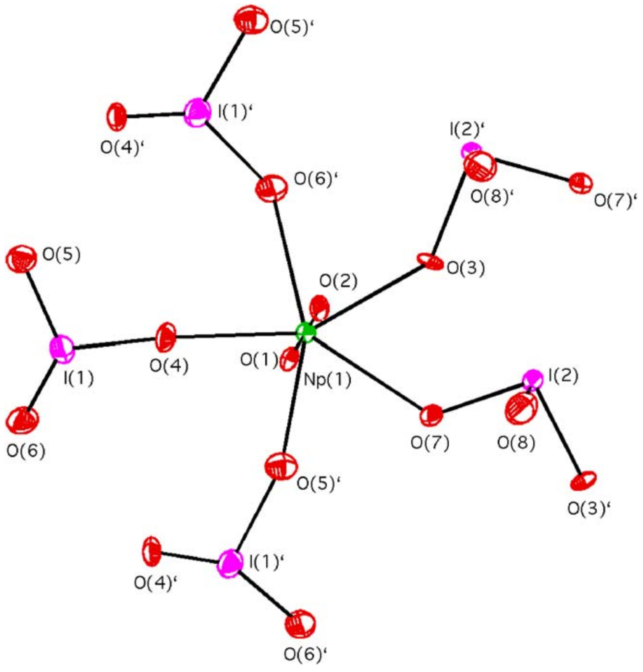

Fig. 2. A depiction of the pentagonal bipyramidal coordination of the Np (can be substituted for Pu) centers in $NpO_2(IO_3)_2 \cdot 0.5KCl \cdot 3.25H_2O$ (**1**) or $PuO_2(IO_3)_2 \cdot 0.5KCl \cdot 2.5H_2O$ (**2**) showing the five equatorial oxygens bound by iodate anions. 50% thermal ellipsoids are depicted.

The *trans*-dioxo cation ($O=An=O$) bond lengths are 1.71(2) and 1.74(2) Å for **1** with an angle of 178.9(6)° and 1.73(2) and 1.74(2) Å for **2** with an angle of 179.1(7)°. The five equatorial oxygen atoms surrounding the metal centers have distances ranging from 2.35(1) to 2.44(1) Å for **1** and 2.36(2) to 2.41(1) Å for **2**, the longest *An*–O distance being shared with a doubly bridging iodate anion. Distances in **1** and **2** compare well with

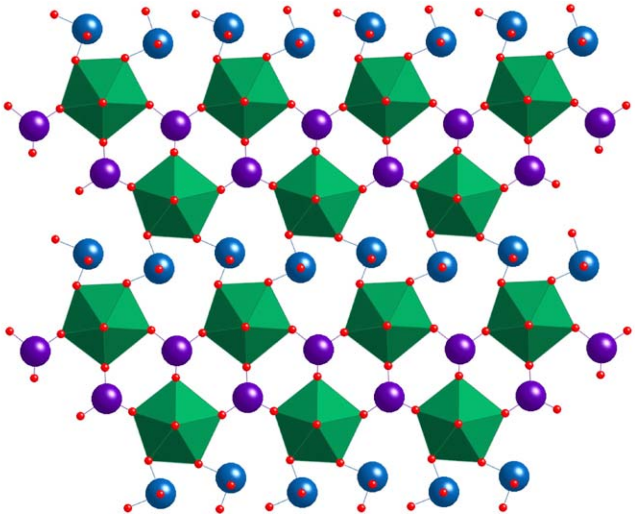

Fig. 3. A view in the *bc*-plane of the neutral sheets in **1** and **2** showing the two different coordinations of the iodate anions. The purple iodate anions are triply bridging while the blue iodate anions are bridging.

those of other hexavalent actinide iodate compounds [11–14,16,17]. Bond valence sum calculations provide a value of 5.97 for Np in **1** [20,21,22].

There are two crystallographically unique iodate anions that occur in different binding modes in **1** and **2**, as shown in Fig. 3. I(1) in **1** and **2** acts as a triply bridging ligand that joins three different actinyl moieties. The I(1)–O distances in **1** range from 1.81(1) to 1.85(1) Å and for **2** occur from 1.80(1) to 1.86(2) Å. The coordination of I(1)–O is not common for the hexavalent actinide iodates but has been found in the trivalent lanthanide iodates, such as $Nd(IO_3)_3 \cdot H_2O$ [23]. In this latter compound the I(1)–O distances range from 1.80(1) to 1.84(2) Å, and are in agreement with those found in **1** and **2**. The second iodine atom, I(2), utilizes only two oxygen atoms to bridge two different actinyl cations to complete the ${}^{2}_{\infty}[AnO_2(IO_3)_2]$ (An = Np, Pu) layers. The I(2)–O distances in **1** range from 1.81(1) to 1.85(2) Å, the longest distance of I(2)–O(8) being the terminal oxygen atom, while in **2**, distances range from 1.83(1) to 1.85(1) Å, with I(2)–O(7) being the longest distance involved in the double bridge. There are close contacts that vary between parallel layers that could account for differences in bonding of I(2). The close contacts in **1** between I(1)·O(8) are ~2.672 Å and in **2** between I(1)·O(8) are ~2.689(1) Å, both of which agree with literature values [11,13,14].

The structural arrangement differs from that of $AnO_2(IO_3)_2 \cdot H_2O$ (An = Np, Pu) [16,17] in that there are two parallel layers separated by water and KCl rather than individual layers, as found in $AnO_2(IO_3)_2 \cdot H_2O$ (An = Np, Pu). The two parallel layers of **1** and **2** are separated by different numbers of waters of hydration. Also present between the layers are K^+ cations and Cl^- anions that form chains, in which the $K^+ \cdots Cl^-$ atoms are separated by a distance of 4.32(1) Å. The KCl chains are not close-packed, as indicated by the $K^+ \cdots Cl^-$ distance, and therefore, allow waters of hydration to fill the void spaces between the layers. The K^+ atoms in **1** and **2** have nearest neighboring water oxygen atoms with average distances of 3.16(2) and 3.134(2) Å, respectively. These distances agree well with those found in other alkali halide chain structures, such as $[RbCl][Cd_6(C_2O_4)_6] \cdot 2H_2O$ and $K_2[Mn_2(C_2O_4)_3]_2[KCl] \cdot 2H_2O$ [24,25], which both have average K–O distances of ~3 Å. Selected bond distances for **1** and **2** are given in Tables 4 and 5.

Table 4
Selected bond distances (Å) for $NpO_2(IO_3)_2 \cdot 0.5KCl \cdot 3.25H_2O$ (**1**)

Np(1) = O(2)	1.705(17)
Np(1) = O(1)	1.739(16)
Np(1)–O(5)′	2.350(14)
Np(1)–O(4)	2.363(14)
Np(1)–O(3)	2.393(13)
Np(1)–O(6)′	2.405(14)
Np(1)–O(7)	2.436(13)
I(1)–O(4)	1.810(14)
I(1)–O(6)	1.826(14)
I(1)–O(5)	1.847(14)
I(2)–O(7)	1.813(13)
I(2)–O(3)′	1.845(12)
I(2)–O(8)	1.852(18)

Table 5
Selected bond distances (Å) for $PuO_2(IO_3)_2 \cdot 0.5KCl \cdot 2.5H_2O$ (**2**)

Pu(1) = O(2)	1.733(16)
Pu(1) = O(1)	1.744(16)
Pu(1)–O(5)′	2.362(15)
Pu(1)–O(4)	2.378(15)
Pu(1)–O(6)′	2.394(15)
Pu(1)–O(3)	2.403(14)
Pu(1)–O(7)	2.418(15)
I(1)–O(4)	1.797(15)
I(1)–O(6)	1.833(15)
I(1)–O(5)	1.857(15)
I(2)–O(7)	1.831(15)
I(2)–O(8)	1.837(17)
I(2)–O(3)′	1.852(14)

4. Conclusions

The number of single crystal structures of neptunium and plutonium is meager in comparison to that of uranium [26]. We have previously shown that neptunium can adopt structure types found for both uranium and plutonium, however in the absence of additional ions, neptunium shows a preference for uranyl topologies [17]. The incorporation of K^+ cations, Cl^- anions, and water molecules changes this trend, and now neptunium conforms to a pluntonyl iodate topology.

In addition, this intercalation of KCl between $^{2}_{\infty}[AnO_2(IO_3)_2]$ (An = Np, Pu) layers demonstrates that these low-dimensional compounds might uptake addition radionuclides present in nuclear waste [27]. Actinide iodates have been shown to be surprisingly resistant to radiation damage [28], and actinyl iodates may therefore mitigate the migration of radionuclides into the environment.

Acknowledgments

This work was supported by the US Department of Energy, Office of Basic Energy Sciences, Heavy Elements Program (Grant DE-FG02-01ER15187). This research was also supported by the Environmental Management Science Program, Office of Science and Technology, US Department of Energy. Los Alamos National Laboratory is operated by the University of California for the US Department of Energy under contact W-7405-ENG-36.

References

[1] H.H. Anderson, in: G.T. Seaborg, J.J. Katz, W.M. Manning (Eds.), The Transuranium Elements. National Nuclear Energy Series, IV, 14B, McGraw-Hill Book Co., New York, 1949, p. 825.

[2] G.R. Hall, R. Hurst, Atomic Energy Research Estab., Harwell, UK, 1957.

[3] D.R. Miller, G.T. Seaborg, S.G. Thompson, US Patent No. 2926067, 1959.

[4] R.W. Stoughton, R.B. Duffield, US Patent No. 2856261, 1958.

[5] P.R. O'Connor, data quoted in Chemical Research, 1944.

[6] J.K. Dawson, R.M. Elliott, The Thermogravimetry of Some Plutonium Compounds, Atomic Energy Research Estab., Harwell, UK, 1953.

[7] D.W. Efurd, W.H. Runde, J.C. Banar, D.R. Janecky, J. Kaszuba, P.D. Palmer, F.R. Roensch, C.D. Tait, Environ. Sci. Technol. 32 (1998) 3893.

[8] J. Kaszuba, W.H. Runde, Environ. Sci. Technol. 33 (1999) 4427.

[9] D.E. Robertson, M.R. Smith, D.W. Koppenaal, R.A. Kiddy, R.S. Strebin, F.P. Brauer, G.A. Ross, D.L. Baldwin, C. Hornibrook, et al., Waste Manage. (Tucson, AZ) 2 (1991) 287.

[10] G.R. Doshi, S.N. Joshi, K.C. Pillai, J. Radioanal. Nucl. Chem. 155 (1991) 115.

[11] A.C. Bean, T.E. Albrecht-Schmitt, J. Solid State Chem. 161 (2001) 146.

[12] A.C. Bean, C.F. Campana, O. Kwon, T.E. Albrecht-Schmitt, J. Am. Chem. Soc. 123 (2001) 8806.

[13] A.C. Bean, S.M. Peper, T.E. Albrecht-Schmitt, Chem. Mater. 13 (2001) 1266.

[14] A.C. Bean, M. Ruf, T.E. Albrecht-Schmitt, Inorg. Chem. 40 (2001) 3959.

[15] A.C. Bean, Y. Xu, J.A. Danis, T.E. Albrecht-Schmitt, W.H. Runde, Inorg. Chem. 41 (2002) 6775.

[16] W.H. Runde, A.C. Bean, T.E. Albrecht-Schmitt, B.L. Scott, Chem. Commun. 4 (2003) 478.

[17] A.C. Bean, B.L. Scott, T.E. Albrecht-Schmitt, W.H. Runde, Inorg. Chem. 42 (2003) 5632.

[18] V. B. A. X.-r. S. Smart: Software for the CCD Detector System, Inc., Madison, WI, 1996. Saint: Software for the CCD Detector System, Version 4.05; Bruker Analytical X-ray Systems, Inc., Madison, WI, 1997. SADABS: Siemens Area Detector Absorption Correction Program, Version 1, 1996.

[19] G.M. Sheldrick SHELXTL PC, Version 5.0, An Integrated System for Solving, Refining, and Displaying Crystal Structures from Diffraction Data. Siemens Analytical X-ray Instruments, Inc., Madison, WI, 1998.

[20] N.E. Brese, M. O'Keeffe, Acta Crystallogr. B 47 (1991) 192.

[21] I.D. Brown, D. Altermatt, Acta Crystallogr. B 41 (1985) 244.

[22] R.E. Sykora, A.C. Bean, B.L. Scott, W.H. Runde, T.E. Albrecht-Schmitt, J. Solid State Chem., 2003, in press.

[23] R. Liminga, S.C. Abrahams, J.L. Bernstein, J. Chem. Phys. 62 (1975) 755.

[24] R. Vaidhyanathan, S. Natarajan, C.N.R. Rao, Chem. Mater. 13 (2001) 3524.

[25] R. Vaidhyanathan, S. Natarajan, C.N.R. Rao, Mater. Res. Bull. 38 (2003) 477.

[26] D.L. Clark, S.D. Conradson, S.A. Ekberg, N.J. Hess, M.P. Neu, P.D. Palmer, W.H. Runde, C.D. Tait, J. Am. Chem. Soc. 118 (1996) 2089.

[27] P.C. Burns, R.C. Ewing, J. Miller, J. Nucl. Mater. 245 (1997) 1.

[28] W.H. Runde, A.C. Bean, B.L. Scott, Chem. Commun. 15 (2003) 1848.